

# PWM Switching Frequency Signal Injection Sensorless Method in IPMSM

Sungmin Kim, Jung-Ik Ha, and Seung-Ki Sul  
Seoul national university Power Electronics Center (SPEC)  
Seoul National University  
Seoul, Korea  
sulsk@plaza.snu.ac.kr

**Abstract**— This paper describes how to extract the rotor position information using a PWM switching frequency voltage signal injection without position sensor in Interior Permanent Magnet Synchronous Machine (IPMSM). The frequency of injected voltage signal is increased to PWM switching frequency, and the dynamics of the sensorless control can be improved. Compared to conventional heterodyning process, the proposed method is simple to implement and appropriate for PWM switching frequency signal injection. The high frequency voltage signal can be injected in the stationary reference frame or in the estimated rotor reference frame. In this paper, two sensorless methods are proposed according to the injection reference frame. To verify the proposed methods, 5kHz voltage signal injection with 5kHz PWM switching frequency inverter system in both reference frames were implemented. The experimental results confirm the effectiveness of the proposed method.

## I. INTRODUCTION

In these days, the popularity of Interior Permanent Magnet Synchronous Machines (IPMSM) has been increased in many industrial drive systems [1]. The high power density, high torque density, and high efficiency are attractive characteristics of IPMSM for not only conventional drive applications but also traction and high performance servo applications. Because IPMSM is a kind of synchronous machine, the rotor position information is essential for field oriented control [2]. As the result, an encoder or resolver has been attached to the shaft of the rotor. These position sensors invoke many problems: increasing system cost and volume, signal noise issues and reliability concerns. Therefore, the control techniques not dependent to the position sensor have been developed for last several decades.

In position sensorless control, there are two groups in the sensorless position estimation of IPMSM according to the position estimation principle. One is based on back EMF, and the other uses the magnetic saliency of IPMSM [3]. In the first group, to extract the rotor position information from the back EMF voltages, it uses voltage models and observers in the synchronous or stationary frame and presents good performance in the middle and high speed operation of IPMSM [4]-[6]. At standstill or very low rotating speed, however, because the voltage from the back EMF, which has

the position information, is proportional to the rotating speed, the signal is too weak to be used as position information. In the second group, rotor position is estimated from the characteristics of IPMSM: the spatial inductance distribution is determined by the rotor position because of the saliency of the magnetic path [7]-[18]. To extract the spatial inductance variation, the relationship between current and voltage is employed. To examine the current-voltage relationship, PWM current ripple can be used [7]-[10]. By measuring of current variation due to the voltage vector variation in one PWM period, inductance can be calculated directly [7]-[9] or estimated with non-linear estimator [10]. However, these methods require the modification of PWM switching pattern, because the current variation in the conventional SVPWM is too small to be used for the calculation of the inductance. And additional equipment to measure the phase currents in arbitrary time should be designed in control hardware, that might not be acceptable to many industry applications. Similarly, the intended discontinuous voltage signal injected method has been proposed [11]. In [11], large voltage signal is injected for very short time interval and the current variation by the injected voltage signal is measured. From measured current variation, the inductance and rotor position can be estimated. However, with this method the rotor position information is obtained discontinuously, the rotor position estimation and the overall control performance would be degraded.

Meanwhile, the continuous voltage signal without PWM modification had been proposed, and the signal can be easily augmented into the conventional current control loop [12]-[18]. The continuous voltage signals into the IPMSM causes the current ripple, which reflects rotor position. From the corresponding current ripple, the rotor position information can be extracted with a properly designed observer and/or state filter. For each signal injection sensorless method, demodulation process should be designed to extract the rotor position related value from current ripple. These signal injection sensorless methods can be further classified into two categories according to where the signal is injected: the rotating voltage signal injection in the stationary reference frame [12], [18] and the pulsating voltage signal injection in the estimated rotor reference frame [13]-[17]. The rotating

voltage signal methods inject the continuous voltage signal spatially regardless of the rotor position, and the pulsating voltage signal methods inject the continuous pulsating voltage signal on the estimated rotor position. These sensorless methods have unique characteristics according to the injected signal type. These characteristics of each sensorless method affect the rotor position detection performance. Many research results have been published the relationships between sensorless methods and their performances.

Generally, the frequency of injected voltage signal is determined between the current control bandwidth and the PWM switching frequency. If the frequency of the injected signal is getting higher, the dynamics of the sensorless control can be enhanced and the interference between the injected signal and the fundamental components of the current control can be diminished. However, the synthesis of the injection voltage by PWM limits the injection frequency up to the PWM switching frequency, ideally, and, furthermore, the filter used in the demodulation process restricts the injection frequency.

In this paper, new sensorless methods for IPMSM drive are proposed to improve the sensorless control performance. This study focus on the highest frequency signal injection. By injecting the voltage signal whose frequency is the same to the PWM switching frequency, which is the theoretical maximum frequency in a drive system fed by a PWM inverter sampling the current twice in a PWM switching period, the injected signal can be easily decoupled from the fundamental frequency and the speed/torque control performance can be enhanced. Moreover, if PWM switching frequency is over the audible range for the most people, which is over 16kHz, the audible noise due to signal injection can be virtually eliminated, which may be a concern with the signal injection in some applications. The proposed signal injection method is compatible to the stationary reference frame or to the estimated rotor reference frame.

## II. BASIC PRINCIPLE OF HIGH FREQUENCY VOLTAGE SIGNAL INJECTION SENSORLESS METHOD

### A. Rotating Voltage Signal Injection in the Stationary Reference Frame

By exploiting the variation of the measured current, the spatial information related to the rotor position can be directly calculated easily. The voltage equation of IPMSM in the stationary d-/q-axis reference frame with currents and flux can be described as (1).

$$\begin{bmatrix} v_{ds}^s \\ v_{qs}^s \end{bmatrix} = R_s \begin{bmatrix} i_{ds}^s \\ i_{qs}^s \end{bmatrix} + \frac{d}{dt} \begin{bmatrix} \lambda_{ds}^s \\ \lambda_{qs}^s \end{bmatrix} \quad (1)$$

where  $[v_{ds}^s, v_{qs}^s]^T$ ,  $[i_{ds}^s, i_{qs}^s]^T$ , and  $[\lambda_{ds}^s, \lambda_{qs}^s]^T$  are the vectors of the stator voltage, current, and flux linkage in the stationary d-/q-axis reference frame, respectively. Physically, the flux linkage in stationary reference frame in (1),  $[\lambda_{ds}^s, \lambda_{qs}^s]^T$ , are function of the stator currents, and the flux linkage of the

rotor permanent magnet. Those flux linkages can be derived as (2).

$$\begin{bmatrix} \lambda_{ds}^s \\ \lambda_{qs}^s \end{bmatrix} = L_s \begin{bmatrix} i_{ds}^s \\ i_{qs}^s \end{bmatrix} + \lambda_f \begin{bmatrix} \cos \theta_r \\ \sin \theta_r \end{bmatrix} \quad (2)$$

where inductance matrix,  $L_s$ , can be represented in terms of d-/q-axis inductances,  $L_{ds}$ ,  $L_{qs}$ , in synchronous rotor reference frame and rotor position,  $\theta_r$ , as (3) and (4).

$$L_s = \begin{bmatrix} \Sigma L + \Delta L \cos 2\theta_r & \Delta L \sin 2\theta_r \\ \Delta L \sin 2\theta_r & \Sigma L - \Delta L \cos 2\theta_r \end{bmatrix} \quad (3)$$

$$\Sigma L = \frac{L_{ds} + L_{qs}}{2} \quad \Delta L = \frac{L_{ds} - L_{qs}}{2} \quad (4)$$

Then, (1) can be represented in terms of by motor parameters and the stator currents as (5).

$$\begin{bmatrix} v_{ds}^s \\ v_{qs}^s \end{bmatrix} = R_s \begin{bmatrix} i_{ds}^s \\ i_{qs}^s \end{bmatrix} + L_s \frac{d}{dt} \begin{bmatrix} i_{ds}^s \\ i_{qs}^s \end{bmatrix} + 2\Delta L \omega_r \begin{bmatrix} -\sin 2\theta_r & \cos 2\theta_r \\ \cos 2\theta_r & \sin 2\theta_r \end{bmatrix} \begin{bmatrix} i_{ds}^s \\ i_{qs}^s \end{bmatrix} + \omega_r \lambda_f \begin{bmatrix} -\sin \theta_r \\ \cos \theta_r \end{bmatrix} \quad (5)$$

where  $\omega_r$  is the rotor speed in electric angle. Because of the saliency of IPMSM, the inductance matrix,  $L_s$ , in (3) has the spatial information of the rotor position. From inductance saliency, the rotor position can be derived by measured current with the voltage signal injection. Under the assumption that the high frequency voltage signal is injected into the IPMSM, the high frequency impedance model of IPMSM can be simply expressed as (6).

$$\begin{bmatrix} v_{dsh}^s \\ v_{qsh}^s \end{bmatrix} = L_s \frac{d}{dt} \begin{bmatrix} i_{dsh}^s \\ i_{qsh}^s \end{bmatrix} \quad (6)$$

where  $[v_{dsh}^s, v_{qsh}^s]^T$ , and  $[i_{dsh}^s, i_{qsh}^s]^T$  are the injected high frequency voltage vector, and current vector in the stationary reference frame, respectively. According to the injected voltage signal, the current response can be derived from (6) as (7).

$$\begin{bmatrix} i_{dsh}^s \\ i_{qsh}^s \end{bmatrix} = \int L_s^{-1} \begin{bmatrix} v_{dsh}^s \\ v_{qsh}^s \end{bmatrix} dt \quad (7)$$

If the voltage signal in (8) shown in Fig. 1(a) is injected to the stationary reference frame, the locus of the voltage vector would a circle as shown in Fig.1(b).

$$v_{dqsh}^s = V_{inj} \begin{bmatrix} -\sin \omega_h t \\ \cos \omega_h t \end{bmatrix} \quad (8)$$

where  $V_{inj}$  and  $\omega_h$  are the amplitude and frequency of the injection signal, respectively. According to this rotating voltage signal, the corresponding current response can be derived from (7) like as

$$\begin{bmatrix} i_{dsh}^s \\ i_{qsh}^s \end{bmatrix} = \frac{V_{inj}}{\Sigma L^2 - \Delta L^2} \begin{bmatrix} \frac{\Sigma L}{\omega_h} \cos \omega_h t + \frac{\Delta L}{2\omega_r - \omega_h} \cos(2\theta_r - \omega_h t) \\ \frac{\Sigma L}{\omega_h} \sin \omega_h t + \frac{\Delta L}{2\omega_r - \omega_h} \sin(2\theta_r - \omega_h t) \end{bmatrix} \quad (9)$$

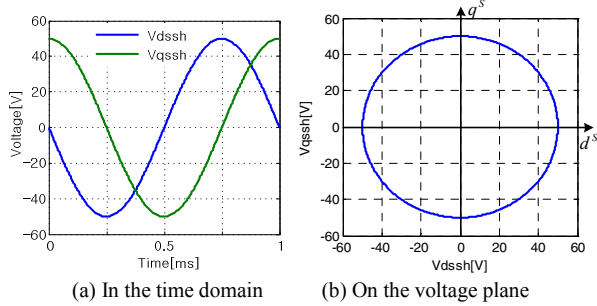


Fig. 1. Conventional rotating voltage vector: amplitude is 50V and the injection frequency is 1kHz. (a) Voltage waveform in the time domain. (b) Locus of injected rotating voltage vector in the stationary reference frame.

From the current response, (9), the rotor position information can be extracted through a kind of signal processing so called as demodulation process. In [12], the heterodyning demodulation process has been proposed as shown in Fig. 2. In this demodulation process, the current responses in (9) are multiplied sinusoidal function whose frequency is identical to the injection frequency. After low-pass-filtering the final result of the demodulation process,  $\varepsilon_f$  in Fig. 2, can be derived as (10).

$$\varepsilon_f \approx \frac{-V_{inj}}{\Sigma L^2 - \Delta L^2} \frac{\Delta L}{\omega_h} 2(\theta_r - \hat{\theta}_r) \quad (10)$$

where the signal injection frequency,  $\omega_h$ , is assumed to be large enough compared to the rotating speed,  $\omega_r$ , ( $\omega_h \gg \omega_r$ ) and the rotor position error between the real position and the estimated position is reasonably small. The process result,  $\varepsilon_f$ , can be used as a corrective error input to Luenberger style observer or state filter as shown in Fig. 2. By driving  $\varepsilon_f$  to zero, the observer or state filter enforces the estimated rotor position to follow the actual rotor position. In Fig. 3, the rotor position estimation result is displayed together with the corresponding current responses through the computer simulation. The parameters for the simulation are the same to the parameters of the experimental set-up, which appear at Table I. in the chapter III.

### B. Pulsating Voltage Signal Injection in the Estimated Rotor Reference Frame

As the rotor position information is derived from the inductance matrix in the stationary reference frame, the rotor position related information can be also extracted from the current-voltage relationship in the estimated rotor reference frame. The voltage equation in the rotor reference frame can be described as (11).

$$\begin{aligned} \begin{bmatrix} v_{ds}^r \\ v_{qs}^r \end{bmatrix} &= R_s \begin{bmatrix} i_{ds}^r \\ i_{qs}^r \end{bmatrix} + \begin{bmatrix} L_{ds} & 0 \\ 0 & L_{qs} \end{bmatrix} \frac{d}{dt} \begin{bmatrix} i_{ds}^r \\ i_{qs}^r \end{bmatrix} \\ &+ \omega_r \begin{bmatrix} 0 & -L_{qs} \\ L_{ds} & 0 \end{bmatrix} \begin{bmatrix} i_{ds}^r \\ i_{qs}^r \end{bmatrix} + \omega_r \lambda_f \begin{bmatrix} 0 \\ 1 \end{bmatrix} \end{aligned} \quad (11)$$

where  $[v_{ds}^r, v_{qs}^r]^T$ , and  $[i_{ds}^r, i_{qs}^r]^T$  are the vectors of the stator voltage, and current in the rotor reference frame, respectively, and  $\lambda_f$  is permanent magnet flux linkage. Supposing the high frequency voltage signal is injected into the IPMSM, the

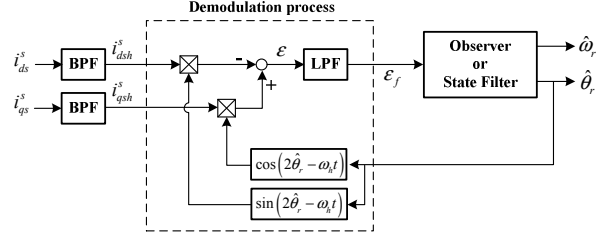
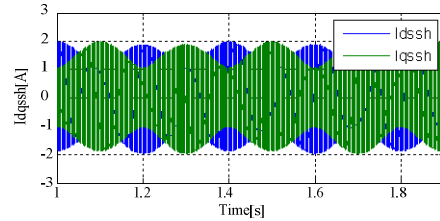
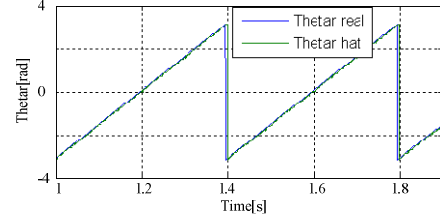


Fig. 2. Block diagram of the heterodyning demodulation process in the rotating voltage vector injection method in the stationary reference frame.



(a) Current response by injection voltage signal



(b) Rotor position estimation result

Fig. 3. Simulation results of the rotating voltage signal injection sensorless method. (a) current response by the injected voltage signal. (b) rotor position estimation result.

high frequency impedance model in the rotor reference frame can be simply described as (12).

$$\begin{bmatrix} v_{dsh}^r \\ v_{qsh}^r \end{bmatrix} = \begin{bmatrix} L_{ds} & 0 \\ 0 & L_{qs} \end{bmatrix} \frac{d}{dt} \begin{bmatrix} i_{dsh}^r \\ i_{qsh}^r \end{bmatrix} \quad (12)$$

where  $[v_{dsh}^r, v_{qsh}^r]^T$ , and  $[i_{dsh}^r, i_{qsh}^r]^T$  are the vector of the injection frequency voltage component, and current component in the rotor reference frame, respectively. According to the injection voltage signal, the current response can be derived from (12) as

$$\begin{bmatrix} i_{dsh}^r \\ i_{qsh}^r \end{bmatrix} = \int \begin{bmatrix} L_{ds} & 0 \\ 0 & L_{qs} \end{bmatrix}^{-1} \begin{bmatrix} v_{dsh}^r \\ v_{qsh}^r \end{bmatrix} dt. \quad (13)$$

In the rotor reference frame sensorless methods, the pulsating voltage signal is injected in the estimated d-axis. Fig. 4 shows the relationship among reference axes. The position error between the real position and the estimated position can be described as

$$\tilde{\theta}_e = \theta_r - \hat{\theta}_r. \quad (14)$$

When the pulsating voltage signal is injected into d-axis in the rotor reference frame, the corresponding current response leads to estimate the rotor position. The pulsating voltage signal in the rotor reference frame is described as

$$\begin{bmatrix} v_{dsh}^r \\ v_{qsh}^r \end{bmatrix} = V_{inj} \begin{bmatrix} \cos \omega_h t \\ 0 \end{bmatrix}. \quad (15)$$

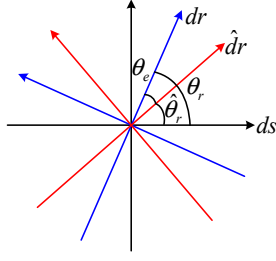


Fig. 4. Relationship between reference axes. Stationary reference frame (black), real rotor reference frame (blue), and estimated rotor reference frame (red).

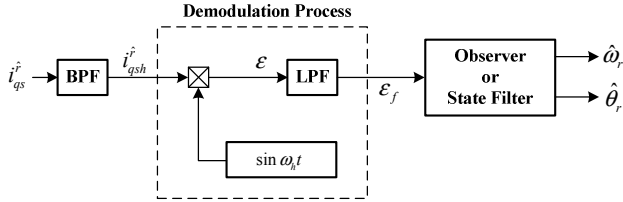


Fig. 5. Block diagram of the heterodyning demodulation process.

Then the corresponding current response can be derived as (16) from (13).

$$\begin{bmatrix} i_{dsh}^r \\ i_{qsh}^r \end{bmatrix} = \frac{V_{inj}}{L_{ds} \omega_h} \begin{bmatrix} \sin \omega_h t \\ 0 \end{bmatrix}. \quad (16)$$

If the pulsating voltage signal is injected into the exact d-axis rotor reference frame, q-axis current ripple does not happen. However, because the exact rotor position is not available, the injection voltage signal actually differs from the ideal injection voltage, (15). The injection voltage in the estimated rotor reference frame can be rewritten with consideration of the estimated rotor position error as (17).

$$V_{dqsh}^r = V_{inj} \begin{bmatrix} \cos \omega_h t \\ 0 \end{bmatrix}. \quad (17)$$

Considering the position error, the actual injection voltage signal into the real rotor reference frame is described as (17).

$$V_{dqsh}^r = T_{\hat{\theta}_r} V_{dqsh}^{\hat{r}} = V_{inj} \begin{bmatrix} \cos \tilde{\theta}_r \cos \omega_h t \\ -\sin \tilde{\theta}_r \cos \omega_h t \end{bmatrix}. \quad (17)$$

where \$T(\tilde{\theta}\_r)\$ stands for the transformation from estimated rotor reference frame to real rotor reference frame. Then, the corresponding current response in the estimated rotor reference frame can be deduced as (19).

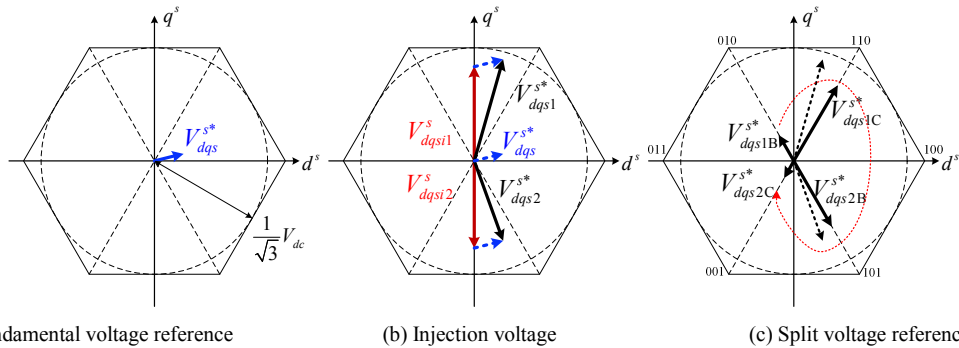
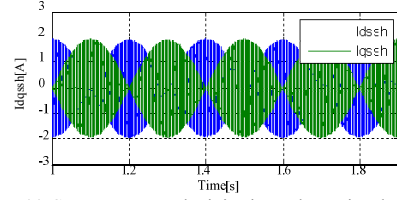
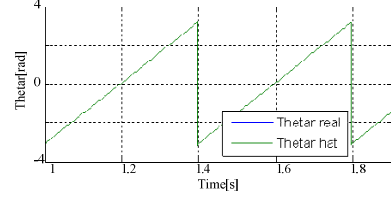


Fig. 7. Modified voltage references at stationary voltage plane.



(a) Current response by injection voltage signal



(b) Rotor position estimation result

Fig. 6. Simulation results of the pulsating voltage signal injection sensorless method. (a) Current response by voltage injection. (b) Rotor position estimation result by demodulation process.

$$\begin{bmatrix} i_{dsh}^r \\ i_{qsh}^r \end{bmatrix} = T_{\hat{\theta}_r}^{-1} \begin{bmatrix} i_{dsh}^r \\ i_{qsh}^r \end{bmatrix} = \frac{V_{inj}}{\omega_h} \begin{bmatrix} \left( \frac{\cos^2 \omega_h t}{L_{ds}} + \frac{\sin^2 \omega_h t}{L_{qs}} \right) \sin \omega_h t \\ \frac{1}{2} \left( \frac{-\Delta L}{L_{ds} L_{qs}} \right) \sin 2\tilde{\theta}_r \sin \omega_h t \end{bmatrix}. \quad (19)$$

It can be seen from (19), the rotor position error is placed in the estimated q-axis current response. Using the heterodyning demodulation process in Fig. 5, the position error can be extracted from q-axis current response. The final result of the demodulation process from the method in Fig. 5, \$\epsilon\_f\$, can be derived as (20).

$$\epsilon_f \approx \frac{1}{2} \frac{V_{inj}}{\omega_h} \left( \frac{-\Delta L}{L_{ds} L_{qs}} \right) (\theta_r - \hat{\theta}_r) \quad (20)$$

where the rotor position error between the real rotor position and the estimated rotor position is assumed to be small. In the same manner as the rotating signal injection method in the previous section, the demodulation process result, \$\epsilon\_f\$, can be used as a corrective error input to observer in Fig. 5 by driving \$\epsilon\_f\$ to zero. In Fig. 6, the rotor position estimation result is displayed together with the corresponding current responses through the computer simulation. The parameters for the computer simulation are the same to the previous case.

### III. PROPOSED PWM SWITCHING FREQUENCY SIGNAL INJECTION SENSORLESS METHODS

By increasing the injection frequency, sensorless system performances as system control bandwidth have been enhanced [15], [16]. In this chapter, the PWM switching frequency voltage signal injection methods are proposed. The proposed methods do not have PWM modification problem and current measurement problem. The high frequency discrete filter is not used in the demodulation process, and the advantages using high frequency signal injection are strengthened. These methods can be implemented in both the stationary reference frame and the estimated rotor reference frame.

#### A. PWM Switching Frequency Signal Injection in the Stationary Reference Frame

The voltage equation can be rewritten as (21), where the derivative of current is expressed in discrete form as current variation ( $\Delta i_{ds}^s, \Delta i_{qs}^s$ ) in a sampling interval,  $\Delta T$ .

$$\begin{bmatrix} v_{ds}^s \\ v_{qs}^s \end{bmatrix} = R_s \begin{bmatrix} i_{ds}^s \\ i_{qs}^s \end{bmatrix} + \omega_r \lambda_f \begin{bmatrix} -\sin \theta_r \\ \cos \theta_r \end{bmatrix} + L_s \frac{1}{\Delta T} \begin{bmatrix} \Delta i_{ds}^s \\ \Delta i_{qs}^s \end{bmatrix} + 2\Delta L \omega_r \begin{bmatrix} -\sin 2\theta_r & \cos 2\theta_r \\ \cos 2\theta_r & \sin 2\theta_r \end{bmatrix} \begin{bmatrix} i_{ds}^s \\ i_{qs}^s \end{bmatrix} \quad (21)$$

In (21), the rotor position information is on the inductance matrix,  $L_s$ . If the inductance matrix can be extracted in (21), the rotor position can be estimated in real time. In [8], the inductance matrix was calculated with high frequency impedance model as (6). Because the inductance matrix,  $L_s$  is a 2 by 2 matrix, two independent voltage vector and current vector have to be used in the calculation. To improve the accuracy in the inductance calculation, the voltage difference method [18] is adapted in the demodulation process. The voltage vector used in the calculation is not the one voltage vector but the voltage difference between two successive voltage vectors. For example, the difference of the voltage vector between two independent voltage vectors,  $(v_{ds1}^s, v_{qs1}^s), (v_{ds2}^s, v_{qs2}^s)$  can be derived by the multiplication inductance matrix,  $L_s$ , and current difference as (22). The inductance matrix can be represented as (23) in terms of two voltage difference vectors. From (23), the rotor position information can be directly calculated as (24).

$$\begin{bmatrix} v_{ds21}^s \\ v_{qs21}^s \end{bmatrix} = \begin{bmatrix} v_{ds2}^s - v_{ds1}^s \\ v_{qs2}^s - v_{qs1}^s \end{bmatrix} = L_s \frac{1}{\Delta T} \begin{bmatrix} \Delta i_{ds2}^s - \Delta i_{ds1}^s \\ \Delta i_{qs2}^s - \Delta i_{qs1}^s \end{bmatrix} = L_s \frac{1}{\Delta T} \begin{bmatrix} \Delta i_{ds21}^s \\ \Delta i_{qs21}^s \end{bmatrix} \quad (22)$$

$$L_s = \Delta T \begin{bmatrix} v_{ds32}^s & v_{ds21}^s \\ v_{qs32}^s & v_{qs21}^s \end{bmatrix} \begin{bmatrix} \Delta i_{ds32}^s & \Delta i_{ds21}^s \\ \Delta i_{qs32}^s & \Delta i_{qs21}^s \end{bmatrix}^{-1} = \begin{bmatrix} L_{11} & L_{12} \\ L_{21} & L_{22} \end{bmatrix} \quad (23)$$

$$2\hat{\theta}_{rCal} = \tan^{-1} \left( \frac{L_{12} + L_{21}}{L_{11} - L_{22}} \right) \quad (24)$$

To get two independent voltage vectors in one PWM switching period, two split PWM switching vectors in a half PWM switching period can be used as shown in Fig. 7. Fundamental voltage reference in Fig. 7(a) means the output

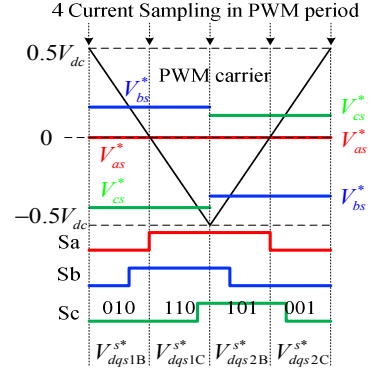


Fig. 8. PWM Sequence with PWM switching voltage injection.

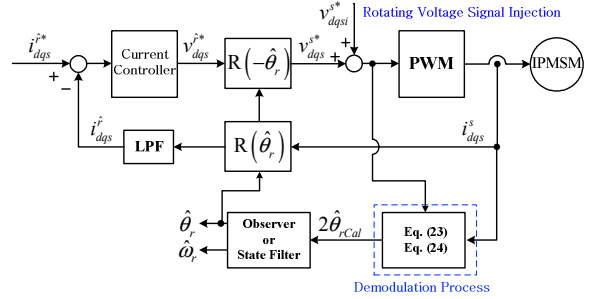


Fig. 9. Block diagram of the proposed rotating voltage signal injection method at PWM switching frequency.

voltage reference of current controller. With injected voltage,  $v_{dqs1}^s$  and  $v_{dqs2}^s$ , the voltage references are modified as  $v_{dqs1}^s$  and  $v_{dqs2}^s$  as shown in Fig. 7(b). The modified voltage references can be split as  $(v_{dqs1}^s \rightarrow v_{dqs1B}^s$  and  $v_{dqs1C}^s)$  and  $(v_{dqs2}^s \rightarrow v_{dqs2B}^s$  and  $v_{dqs2C}^s)$  in PWM period as Fig. 7(c). Therefore, four voltage vectors which induce the additional current ripple can be obtained in every PWM switching period. Even though the fluctuating voltage signal at the fixed axis is injected where positive voltage and negative voltage are added in the on and off sequences, respectively, the voltage vectors by SVPWM are implemented to be the rotated ones as in Fig. 7(c). To calculate the inductance matrix,  $L_s$ , the corresponding current according to the each voltage vector should be measured. In Fig. 8 the sequence related to the voltage vectors and corresponding sampled currents are displayed.

To use the four voltage vectors and the corresponding current values, the split voltage vectors  $(v_{dqs1B}^s, v_{dqs1C}^s)$  and  $(v_{dqs2B}^s, v_{dqs2C}^s)$  have to change from  $v_{dqs1B}^s$  to  $v_{dqs1C}^s$  and from  $v_{dqs2B}^s$  to  $v_{dqs2C}^s$  at the center of the half PWM switching period as shown in Fig. 8. By so doing, the current measurement instant is fixed as the center in a half of PWM period. This PWM sequence can be easily implemented using carrier based offset voltage PWM concept in [19]. To extract the position information, the voltage and current vectors which are used in the calculation are derived as (25) in the manner of (22). The inductance matrix can be determined as (26) and the rotor position can be finally calculated as (24) from (26).

$$\begin{bmatrix} v_{ds1BC}^s \\ v_{qs1BC}^s \end{bmatrix} = \begin{bmatrix} v_{ds1B}^s - v_{ds1C}^s \\ v_{qs1B}^s - v_{qs1C}^s \end{bmatrix} = L_s \frac{1}{\Delta T} \begin{bmatrix} \Delta i_{ds1B}^s - \Delta i_{ds1C}^s \\ \Delta i_{qs1B}^s - \Delta i_{qs1C}^s \end{bmatrix} = L_s \frac{1}{\Delta T} \begin{bmatrix} \Delta i_{ds1BC}^s \\ \Delta i_{qs1BC}^s \end{bmatrix}. \quad (25)$$

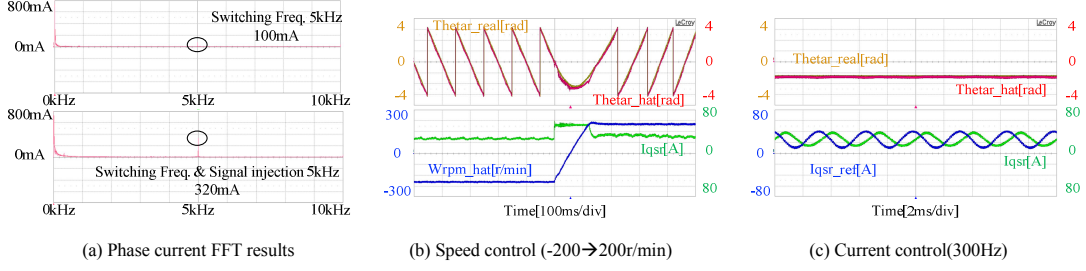


Fig. 10. Rotating signal injection sensorless control performance.

$$L_S = \Delta T \begin{bmatrix} \gamma_{ds2BC}^s & \gamma_{ds1BC}^s \\ \gamma_{qs2BC}^s & \gamma_{qs1BC}^s \end{bmatrix} \begin{bmatrix} \Delta i_{ds2BC}^s & \Delta i_{ds1BC}^s \\ \Delta i_{qs2BC}^s & \Delta i_{qs1BC}^s \end{bmatrix}^{-1} = \begin{bmatrix} L_{11} & L_{12} \\ L_{21} & L_{22} \end{bmatrix}. \quad (26)$$

The overall block diagram of the proposed rotating voltage injection sensorless method in the stationary reference frame is shown in Fig. 9. In the current feedback loop, the low-pass-filter still exists. However, because the frequency of current ripple is PWM switching frequency, the low-pass-filter is very weak and the cut-off frequency can be increased up to a half of PWM switching frequency.

To verify the proposed sensorless method, as a test set-up, an 11kW IPMSM drive system coupled to a load machine was used. IPMSM parameters and the drive system parameters are listed in Table I. PWM switching frequency is 5kHz, and the current sampling frequency for current control is 10kHz. For sensorless operation, currents are measured two times in one PWM period. The current signal due to the injected voltage signal is shown in lower figure of Fig. 10(a). In Fig. 10(b) the speed control performance under speed reference variation from -200r/min to 200r/min with load is demonstrated. To show the current regulation performance, the results of a current regulation according to 300Hz sinusoidal current reference with a positive offset was displayed in Fig. 10(c). Because the injection frequency is PWM switching frequency, 5kHz, the 300Hz current reference does not degrade the rotor position tracking performance, at all even with this relatively high current regulation bandwidth.

TABLE I. PARAMETERS OF IPMSM AND DRIVE SYSTEM

	Item	Quantity
IPMSM Parameter	Rated Power	11kW
	Rated Speed	1750r/min
	Rated current	39.5Arms
	Stator Resistance	0.14Ω
	Nominal Inductance	$L_{ds}: 3.4\text{mH} / L_{qs}: 4.3\text{mH}$
	PM Flux linkage	$\lambda_f: 0.253\text{V}\cdot\text{s}/\text{rad}$
System Parameter	DC-link Voltage	310V
	PWM Switching Freq.	5kHz
	Current Sampling Freq.	10kHz
	Current Control Bandwidth	300Hz
	Speed Control Bandwidth	25Hz

### B. Pulsating Voltage Signal Injection in the Estimated Rotor Reference Frame

In the same way of previous section, the current ripple due to the pulsating voltage signal in the estimated rotor reference frame can be calculated using the measured current difference. Eq. (27) describes the voltage equation of IPMSM in the d-/q-axis rotor reference frame.

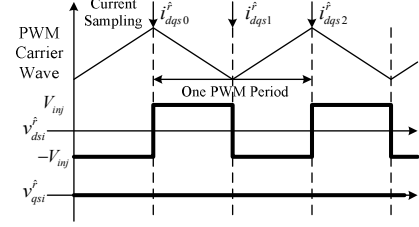


Fig. 11. Pulsating injection voltage signal in the estimated rotor reference frame. In one PWM period, three successive measured currents are used to estimate the rotor position.

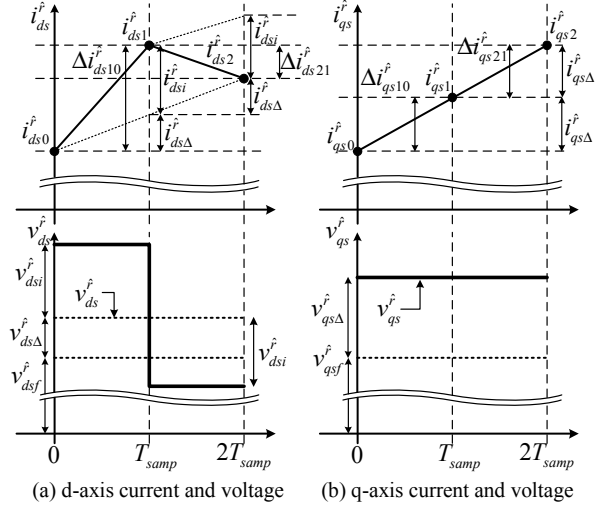


Fig. 12. Estimated rotor reference frame voltage signal injection. (a) d-axis voltage reference and injected signal in a PWM period and the corresponding current response. (b) q-axis voltage reference and the corresponding current response.

$$\begin{bmatrix} v_{ds}^f \\ v_{qs}^f \end{bmatrix} = R_s \begin{bmatrix} i_{ds}^f \\ i_{qs}^f \end{bmatrix} + \begin{bmatrix} L_{ds} & 0 \\ 0 & L_{qs} \end{bmatrix} \frac{1}{\Delta T} \begin{bmatrix} \Delta i_{ds}^s \\ \Delta i_{qs}^s \end{bmatrix} + \omega_r \left( \begin{bmatrix} 0 & -L_{qs} \\ L_{ds} & 0 \end{bmatrix} \begin{bmatrix} i_{ds}^f \\ i_{qs}^f \end{bmatrix} + \begin{bmatrix} 0 \\ \lambda_f \end{bmatrix} \right) \quad (27)$$

To estimate the rotor position, the pulsating voltage signal of which frequency is PWM switching frequency can be injected as Fig. 11. At the only d-axis in the estimated rotor reference frame, the square wave signal is injected, and the currents are measured two times for every PWM period. This high frequency voltage signal causes the same frequency current ripples based on the high frequency inductance model of IPMSM as (28). Because the high frequency signal is injected on the estimated rotor reference frame, the voltage signal in the real rotor reference frame is transformed with position error. By voltage signal in (29), the current ripple in (30) can be derived from (28). In the same manner, the currents can be only measured in the estimated rotor reference frame as (31).

$$\begin{bmatrix} v_{dsh}^r \\ v_{qsh}^r \end{bmatrix} = \begin{bmatrix} L_{ds} & 0 \\ 0 & L_{qs} \end{bmatrix} \frac{1}{\Delta T} \begin{bmatrix} \Delta i_{dsh}^r \\ \Delta i_{qsh}^r \end{bmatrix}. \quad (28)$$

$$V_{dqsh}^r = T_{\tilde{\theta}_r} V_{dqsh}^{\hat{r}} = \pm V_{inj} \begin{bmatrix} \cos \tilde{\theta}_r \\ -\sin \tilde{\theta}_r \end{bmatrix}. \quad (29)$$

$$\begin{bmatrix} \Delta i_{dsh}^r \\ \Delta i_{qsh}^r \end{bmatrix} = \pm \Delta T \cdot V_{inj} \begin{bmatrix} 1/L_{ds} \cos \tilde{\theta}_r \\ -1/L_{qs} \sin \tilde{\theta}_r \end{bmatrix}. \quad (30)$$

$$\begin{bmatrix} \Delta i_{dsh}^{\hat{r}} \\ \Delta i_{qsh}^{\hat{r}} \end{bmatrix} = T_{\tilde{\theta}_r}^{-1} \begin{bmatrix} \Delta i_{dsh}^r \\ \Delta i_{qsh}^r \end{bmatrix} = \pm \Delta T \cdot V_{inj} \begin{bmatrix} \frac{\cos^2 \tilde{\theta}_r}{L_{ds}} + \frac{\sin^2 \tilde{\theta}_r}{L_{qs}} \\ \frac{1}{2} \left( \frac{1}{L_{ds}} - \frac{1}{L_{qs}} \right) \sin 2\tilde{\theta}_r \end{bmatrix}. \quad (31)$$

Theoretically, the rotor position error information is placed on the q-axis current ripple in the estimated rotor reference frame as (31). Therefore, the estimated q-axis current ripple can be used as the rotor position error value for sensorless control.

When the voltage references which are the output of fundamental current controller and the injected pulsating voltages are determined as shown in Fig. 11, the current ripple only due to the injected voltage signal can be calculated easily. Fig. 12 shows the voltage reference and the corresponding current response. The d-/q-axis voltage references (32) from current control loop consist of two components: fundamental voltage as (33) and current control voltage as (34). The current control voltages mean the portion of the voltage reference, which cause the current variation.

$$v_{ds}^{\hat{r}} = v_{dsf}^{\hat{r}} + v_{dsc}^{\hat{r}} = R_s i_{ds}^{\hat{r}} - \omega_r L_{qs} i_{qs}^{\hat{r}} + L_{ds} \frac{di_{ds}^{\hat{r}}}{dt} \quad (32)$$

$$v_{qs}^{\hat{r}} = v_{qsf}^{\hat{r}} + v_{qsc}^{\hat{r}} = R_s i_{qs}^{\hat{r}} + \omega_r L_{ds} i_{ds}^{\hat{r}} + \omega_r \lambda_f + L_{qs} \frac{di_{qs}^{\hat{r}}}{dt}$$

$$\begin{aligned} v_{dsf}^{\hat{r}} &= R_s i_{ds}^{\hat{r}} - \omega_r L_{qs} i_{qs}^{\hat{r}} \\ v_{qsf}^{\hat{r}} &= R_s i_{qs}^{\hat{r}} + \omega_r L_{ds} i_{ds}^{\hat{r}} + \omega_r \lambda_f \end{aligned} \quad (33)$$

$$v_{dsc}^{\hat{r}} = L_{ds} \frac{di_{ds}^{\hat{r}}}{dt} \quad v_{qsc}^{\hat{r}} = L_{qs} \frac{di_{qs}^{\hat{r}}}{dt}. \quad (34)$$

However, when the voltage signals are added, the current ripples occur by two voltages: the current control voltage and the injection voltage. For the rotor position estimation, the current ripple due to only the injected voltage signal should be extracted from the current ripples. Fig. 12 shows the voltage references and the corresponding current ripples. For one PWM period, the estimated d-/q-axis current variation are  $2i_{ds\Delta}^{\hat{r}}$  and  $2i_{qs\Delta}^{\hat{r}}$ , respectively, and the current ripples by the injection signal are  $i_{dsi}^{\hat{r}}$  and  $i_{qsi}^{\hat{r}}$ . The current ripples due to only the injection signal can be obtained from the three successive measured currents. The current ripple in the first half PWM period consists of the fundamental current ripple,

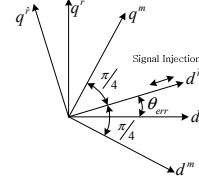


Fig. 13. Real axis, estimated axis and measurement axis in the rotor reference frame.

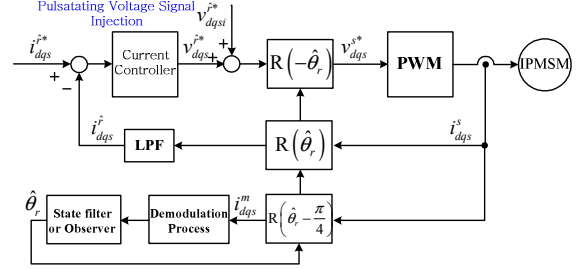


Fig. 14. Block diagram of the proposed pulsating voltage signal injection method with the switching frequency signal injection.

$i_{dqs\Delta}^{\hat{r}}$ , and injection signal current ripple,  $i_{dqsi}^{\hat{r}}$  as (35). In the second half PWM period, the current ripples can be analyzed as (36). Therefore, the current ripple due to the only injection signal can be obtained as difference between current ripples in two half PWM periods as (37).

$$\begin{aligned} \Delta i_{ds10}^{\hat{r}} &= i_{ds1}^{\hat{r}} - i_{ds0}^{\hat{r}} = i_{ds\Delta}^{\hat{r}} + i_{dsi}^{\hat{r}} \\ \Delta i_{qs10}^{\hat{r}} &= i_{qs1}^{\hat{r}} - i_{qs0}^{\hat{r}} = i_{qs\Delta}^{\hat{r}} + i_{qsi}^{\hat{r}} \end{aligned} \quad (35)$$

$$\begin{aligned} \Delta i_{ds21}^{\hat{r}} &= i_{ds2}^{\hat{r}} - i_{ds1}^{\hat{r}} = i_{ds\Delta}^{\hat{r}} - i_{dsi}^{\hat{r}} \\ \Delta i_{qs21}^{\hat{r}} &= i_{qs2}^{\hat{r}} - i_{qs1}^{\hat{r}} = i_{qs\Delta}^{\hat{r}} - i_{qsi}^{\hat{r}} \end{aligned} \quad (36)$$

$$\begin{aligned} \Delta i_{ds10}^{\hat{r}} - \Delta i_{ds21}^{\hat{r}} &= 2i_{dsi}^{\hat{r}} \\ \Delta i_{qs10}^{\hat{r}} - \Delta i_{qs21}^{\hat{r}} &= 2i_{qsi}^{\hat{r}} \end{aligned} \quad (37)$$

From (31), the calculated current ripple can be physically rewritten as (38). The rotor position error between the real rotor position and the estimated rotor position can be also obtained by other demodulation process in [14]. To extract the position error from current ripple, the orthogonal measurement axes, the  $d^m$  and  $q^m$ -axis shown in Fig.13 is used [14]. The difference between the  $d^m$ -axis current ripple and  $q^m$ -axis current ripple is proportional to the rotor position error between the real rotor position and the estimated rotor position as (40).

$$\begin{bmatrix} i_{dsi}^{\hat{r}} \\ i_{qsi}^{\hat{r}} \end{bmatrix} = \begin{bmatrix} \Delta i_{ds10}^{\hat{r}} - \Delta i_{ds21}^{\hat{r}} \\ \Delta i_{qs10}^{\hat{r}} - \Delta i_{qs21}^{\hat{r}} \end{bmatrix} = 2\Delta T \cdot V_{inj} \begin{bmatrix} \frac{\cos^2 \tilde{\theta}_r}{L_{ds}} + \frac{\sin^2 \tilde{\theta}_r}{L_{qs}} \\ \frac{1}{2} \left( \frac{1}{L_{ds}} - \frac{1}{L_{qs}} \right) \sin 2\tilde{\theta}_r \end{bmatrix}. \quad (38)$$

$$\begin{bmatrix} i_{dsi}^m \\ i_{qsi}^m \end{bmatrix} = \pm \frac{\Delta T \cdot V_{inj}}{\sqrt{2}} \begin{bmatrix} \frac{\cos^2 \tilde{\theta}_r}{L_{ds}} + \frac{\sin^2 \tilde{\theta}_r}{L_{qs}} - \frac{1}{2} \left( \frac{1}{L_{ds}} - \frac{1}{L_{qs}} \right) \sin 2\tilde{\theta}_r \\ \frac{\cos^2 \tilde{\theta}_r}{L_{ds}} + \frac{\sin^2 \tilde{\theta}_r}{L_{qs}} + \frac{1}{2} \left( \frac{1}{L_{ds}} - \frac{1}{L_{qs}} \right) \sin 2\tilde{\theta}_r \end{bmatrix}. \quad (39)$$

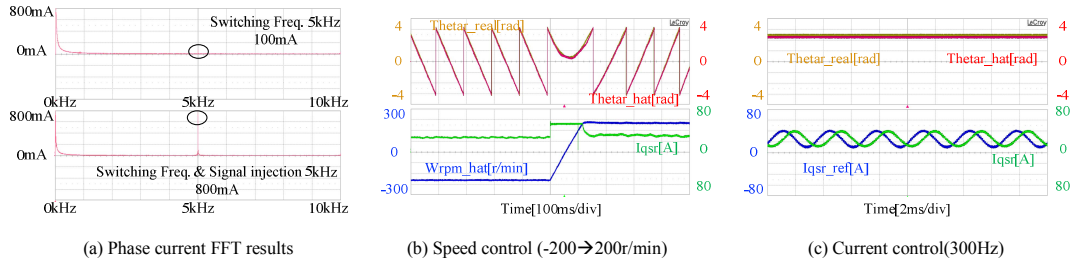


Fig. 15. Pulsating signal injection sensorless control performance.

$$\tilde{\theta}_r = K \left( |i_{qsi}^m| - |i_{dsi}^m| \right). \quad (40)$$

With a state filter or an observer, the rotor position can be estimated through (40). The entire control block diagram of the pulsating signal injection sensorless method with the switching frequency signal injection is shown in Fig. 14.

To verify the proposed pulsating signal injection sensorless method, the same test set-up of the case of the rotating signal injection to the stationary reference frame. PWM switching frequency is 5kHz and current sampling frequency is 10kHz. The frequency spectrum of current signal due to the injected voltage signal is shown in lower figure of Fig. 15(a). In Fig. 15(b), it is shown that the speed control performance under speed reference change from -200r/min to 200r/min with load, and the current regulation performance was demonstrated in Fig. 15(c). The results are almost same to the results in the Fig. 10.

#### IV. CONCLUSION

This paper presented PWM switching frequency signal injection sensorless method for an IPMSM drive. To extract the current ripple component according to the injected voltage signal, the current difference between voltage vectors are used for the simple calculation. To inject the switching frequency rotating voltage signal into IPMSM, the PWM pattern was modified with the carrier based PWM method. Because of this high injection frequency, the dynamics of the sensorless control can be enhanced. The proposed method can be applied to both stationary reference frame injection and the estimated rotor reference frame injection. Though the experimental results are obtained at 5kHz PWM switching frequency because of the limited resources of the experimental set-up, the possibility of the elimination of the acoustic noise due to signal injection can open up by the proposed PWM switching frequency signal injection method under the condition of high enough PWM switching frequency.

#### REFERENCES

- [1] N. Bianchi, and T. M. Jahns, *Design, Analysis, and control of Interior PM Synchronous Machines*, Tutorial course notes of IAS2004, 2004.
- [2] P. Vas, *Sensorless vector and direct torque control*, Oxford, 1998, pp. 122-124.
- [3] J.-I. Ha, K. Ide, T. Sawa, and S.-K. Sul, "Sensorless rotor position estimation of an interior permanent-magnet motor from initial states," *IEEE Trans. Ind. Appl.*, vol. 39, no. 3, pp. 761-767, May/June 2003.
- [4] N. Matsui, "Sensorless operation of brushless DC motor drives," in *Proc. IEEE IECON'93*, 1993, pp. 739-744.
- [5] S. Morimoto, K. Kawamoto, M. Sanada, and Y. Takeda, "Sensorless control strategy for salient-pole PMSM based on extended EMF in rotating reference frame," *IEEE Trans. Ind. Appl.*, vol. 38, no. 4, pp. 1054-1061, Jul./Aug. 2002.
- [6] B.-H. Bae, S.-K. Sul, J.-H. Kwon, and J.-S. Byeon, "Implementation of sensorless vector control for super-high-speed PMSM of turbo-compressor," *IEEE Trans. Ind. Appl.*, vol. 39, no. 3, pp. 811-818, May/June 2003.
- [7] A. B. Kulkarni, and M. Ehsani, "A novel position sensor elimination technique for the interior permanent-magnet synchronous motor drive," *IEEE Trans. Ind. Appl.*, vol. 28, no. 1, pp. 144-170, Jan./Feb. 1992.
- [8] S. Ogasawara, and H. Akagi, "Implementation and position control performance of a position-sensorless IPM motor drive system based on magnetic saliency," *IEEE Trans. Ind. Appl.*, vol. 34, pp. 806-812, Jul./Aug. 1998.
- [9] M. Mamo, K. Ide, M. Sawamura, and J. Oyama, "Novel rotor position extraction based on carrier frequency component method (FCFM) using two reference frames for IPM drives," *IEEE Trans. Ind. Electron.*, vol. 52, no. 5, pp. 508-514, Apr. 2005.
- [10] V. Petrovic, A. M. Stankovic, and V. Blasko, "Position estimation in salient PM synchronous motors based on PWM excitation transients," *IEEE Trans. Ind. Appl.*, vol. 39, no. 3, pp. 835-843, May/June 2003.
- [11] M. Schroedl, "Sensorless control of AC machine at low speed and standstill based on the 'INFORM' method," in *Conf. Rec. IEEE-IAS Annu. Meeting*, 1996, pp. 270-277.
- [12] P. L. Jansen, and R. D. Lorenz, "Transducerless position and velocity estimation in induction and salient AC machines," *IEEE Trans. Ind. Appl.*, vol. 31, no. 2, pp. 240-247, Mar./Apr. 1995.
- [13] M. J. Corley, and R. D. Lorenz, "Rotor position and velocity estimation for a salient-pole permanent magnet synchronous machine at standstill and high speeds," *IEEE Trans. Ind. Appl.*, vol. 34, no. 4, pp. 784-789, Jul./Aug. 1998.
- [14] J.-I. Ha, and S.-K. Sul, "Sensorless field-orientation control of an induction machine by high-frequency signal injection," *IEEE Trans. Ind. Appl.*, vol. 35, no. 1, pp. 45-51, Jan./Feb. 1999.
- [15] R. Leidhold, and P. Mutschler, "Improved method for higher dynamics in sensorless position detection," in *Proc. IEEE IECON2008*, 2008, pp. 1240-1245.
- [16] Y.-D. Yoon, S.-K. Sul, S. Morimoto, and K. Ide, "High bandwidth sensorless algorithm for AC machines based on square-wave-type voltage injection," *IEEE Trans. Ind. Appl.*, vol. 47, no. 3, pp. 1361-1370, May/June 2011.
- [17] R. Masaki, S. Kaneko, M. Hombu, T. Sawada, and S. Yoshihara, "Development of a position sensorless control system on an electric vehicle driven by a permanent magnet synchronous motor," in *Proc. IEEE PCC Osaka 2002*, vol. 2, 2002, pp. 571-576.
- [18] S. Kim, Y.-C. Kwon, S.-K. Sul, J. Park, and S.-M. Kim, "Position sensorless operation of IPMSM with near PWM switching frequency signal injection," in *Proc. of ICPE2011-ECCE Asia*, 2011.
- [19] D.-W. Chung, J.-S. Kim and S.-K. Sul, "Unified voltage modulation technique for real-time three-phase power conversion," *IEEE Trans. Ind. Appl.*, vol. 34, no. 2, pp. 374-380, Mar./Apr. 1998.